EFFECT OF SECONDARY AIR ON SOOT NUCLEUS PRODUCTION IN STOKER-FIRED BOILERS

by

Qing-Cheng WANG[a]* and Zhao-Chun WU[a]

[a] School of City Construction and Safety Engineering, Shanghai Institute of Technology, Shanghai, China

Original scientific paper
DOI: 10.2298/TSCI1305317W

Black smoke emission and soot nucleus production in a stoker-fired boiler by secondary air are studied numerically and experimentally. Temperature field, flow field, and soot nucleus concentration are predicted numerically. It reveals that the secondary air gives about 10% reduction of the soot nucleus production, and the black smoke emission is controlled evidently.

Key words: *soot nucleus, gas flow, secondary air, temperature field, simulation*

Introduction

The soot particle derived from coal combustion affects the environmental quality and people's health, causes people's acute and chronic diseases [1, 2], so it is has been caught much attention. Soot nucleus is foundation of soot formation. Up to now, many works focus on the soot formation derived from simply gas hydrocarbons, liquid fuels and pulverized coals [3], however few works were done for soot formation and soot nucleus production derived from lump-coal combustion in a stoker-fired boiler. There are more than 0.5 million industrial boilers and the total installed capacity of the industrial boilers is more than 1.2 million tons per hour; more than 400 million tons of coals are consumed in China; and the stoker-fired boiler is the dominating combustion style. The characters of this boiler style are low in efficiency and high in pollutants emission. It is significant to simulate soot nucleus generation in order to reduce the soot emission and to increase the efficiency of a stoker-fired boiler [4-7].

Simulation method

Computation model

The computation model [8-10] used in this paper is:

k-ε model

$$\frac{\partial}{\partial x_i}(u_i) = 0 \tag{1}$$

$$\rho \frac{\mathrm{D}u_i}{\mathrm{D}t} = -\frac{\partial p}{\partial x_i} + \frac{\partial}{\partial x_j}\left[\mu_e\left(\frac{\partial u_i}{\partial x_j} + \frac{\partial u_j}{\partial x_i}\right)\right] + \rho g_i \tag{2}$$

* Corresponding author; e-mail: wangqc@sit.edu.cn

$$\rho\frac{\mathrm{D}k}{\mathrm{D}t}=\frac{\partial}{\partial x_j}\left[\left(\mu+\frac{\mu_T}{\sigma_k}\right)\frac{\partial k}{\partial x_j}\right]+G_k-\rho\varepsilon \tag{3}$$

$$\rho\frac{\mathrm{D}\varepsilon}{\mathrm{D}t}=\frac{\partial}{\partial x_j}\left[\left(\mu+\frac{\mu_T}{\sigma_\varepsilon}\right)\frac{\partial \varepsilon}{\partial x_j}\right]+c_1\frac{\varepsilon}{k}G_k-c_2\rho\frac{\varepsilon^2}{k} \tag{4}$$

$$\frac{\partial}{\partial t},(\rho H)+\frac{\partial}{\partial x_i}(\rho u_i H)=\frac{\partial}{\partial x_i}\left(\frac{k_i}{c_p}\frac{\partial H}{\partial x_i}\right)+\tau_{ik}\frac{\partial u_i}{\partial x_i}+S_h \tag{5}$$

where $\mu_T=\rho c_\mu\dfrac{k^2}{\varepsilon}$, $\mu_e=\mu+\mu_T$, $G_k=-\rho\overline{u_i'u_j'}\dfrac{\partial u_j}{\partial x_i}$, c_1 = 1.44, c_2 = 1.92, c_μ = 0,09, σ_k = 1.0, and σ_ε = 1.3.

Combustion model

$$\frac{\partial}{\partial t}(\rho\bar{f})+\nabla\cdot(\rho\bar{v}\bar{f})=\nabla\cdot\left(\frac{\mu_t}{\sigma_t}\nabla\bar{f}\right)+s_m+s_{\text{user}} \tag{6}$$

$$\frac{\partial}{\partial t}\left(\rho\overline{f'^2}\right)+\nabla\cdot\left(\rho\bar{v}\overline{f'^2}\right)=\nabla\cdot\left(\frac{\mu_t}{\sigma_t}\nabla\overline{f'^2}\right)+c_g\mu_t\left(\nabla^2\bar{f}\right)-c_d\rho\frac{\varepsilon}{k}\overline{f'^2}+s_{\text{user}} \tag{7}$$

where f is the mixed fraction, constant σ_t = 0.85, c_g = 2.86, and c_d = 2.0.

Radiation model

$$-\nabla q_r=aG-4a\sigma T^4 \tag{8}$$

Soot Tesner model

$$\frac{\partial}{\partial t}\left(\rho b^*_{\text{nuc}}\right)+\nabla\cdot\left(\rho\vec{v}b^*_{\text{nuc}}\right)=\nabla\cdot\left(\frac{\mu_t}{\sigma_{\text{nuc}}}\nabla b^*_{\text{nuc}}\right)+R^*_{\text{nuc}} \tag{9}$$

where b^*_{nuc} – the soot nucleus concentration, σ_{nuc} – the turbulent Prandtl number for soot nucleus transport, R^*_{nuc} – the net rate of soot nucleus generation, is the balance of soot nucleus formation and soot combustion.

Computation method

The height and width of computation area is 1000 mm and 200 mm, respectively, which are divided into 108365 meshes. The computation method is Semi-Implicit Method for Pressure Linked Equation Consistent (SIMPLE). Inlet boundary conditions of fuel refer to testing result of volatiles in stoker-fired boiler. Methane, acetylene, and benzene, are related to soot formation. Inlet air velocity is 0.175-0.788 m/s. Excess air factor is 1.05. Secondary air velocity is 0.98 m/s.

Simulation result

Influence on temperature field in hearth without and with secondary air

Temperature field is described as fig. 1. High temperature area in hearth concentrates in the area over coal bed when no secondary air is injected to the hearth; on the other

hand, high temperature in hearth concentrate in the area over coal bed and the secondary air injection area when the secondary air is injected to the hearth. The combustion of volatile and char releases heat. The high temperature zone over coal bed is due to the volatile and char combustion; and the high temperature zone in the secondary injection area is due to part of volatile and secondary air mixing and combustion. The highest temperature in hearth is 1680 K and 1670 K because of the normal secondary air convection influence. The highest temperature varies imperceptibly and the high temperature area is increased, taking account of the secondary air injection.

Influence on flow field in hearth without and with secondary air

Flow field is presented as fig. 2. High-velocity flue gases are mainly concentrated in the area over coal bed without secondary air injection to the hearth; from another point of view, high-velocity flue gases are mainly concentrated in the area over coal bed and the secondary injection area with secondary air injection to the hearth. The high-velocity flue gases over coal bed are due to volatile and primary air injection; the high-velocity flue gases in secondary injection area are due to the secondary air injection disturbing the flue gases nearby. The highest velocity of flue gases is 2.01 m/s and 2.50 m/s without secondary air and with secondary air separately because of the secondary air disturbance.

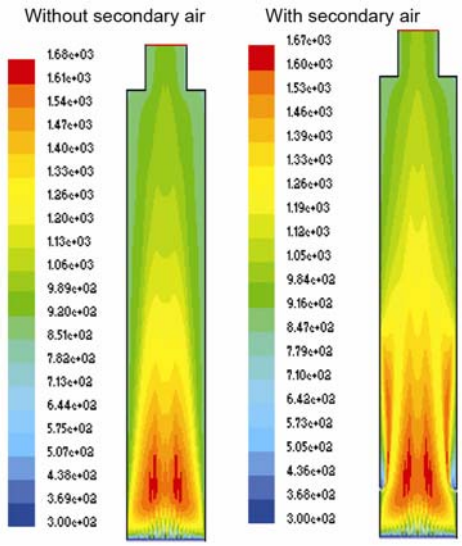

Figure 1. Temperature field distribution in hearth without and with secondary air
(for color image see journal web site)

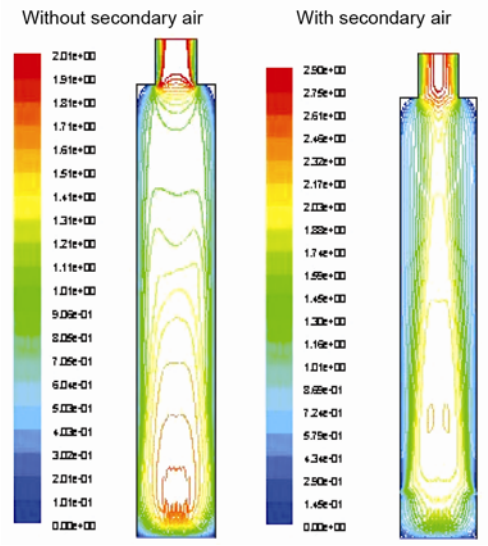

Figure 2. Flow field distribution in hearth without and with secondary air
(for color image see journal web site)

Soot nucleus production without and with secondary air

Soot nucleus production without secondary air

Soot nucleus mass concentration is expressed as the left column in fig. 3. The highest mass concentration is $6.65 \cdot 10^{-11}$%. Soot nucleus mass concentration is high in the area where the volatile concentration is high because volatile are not burned out in time and

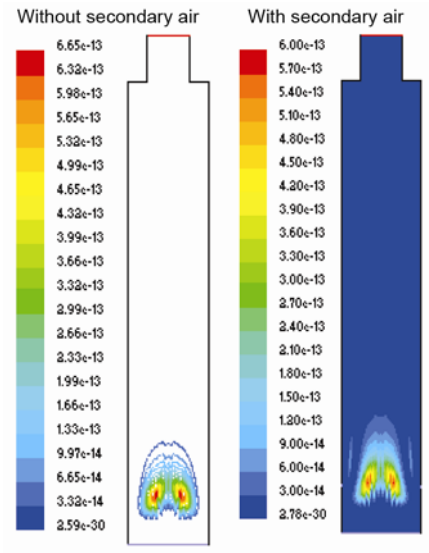

Figure 3. Mass fraction of soot nucleus in furnace without and with secondary air
(for color image see journal web site)

formed soot nucleus. Soot nucleus mass concentration is high in the area where the temperature is high and the oxygen is shortage.

Soot concentration with secondary air

Soot nucleus mass concentration is expressed as the right column in fig. 3. The highest mass concentration is $6.00 \cdot 10^{-11}$%, which is lower than that without secondary air. Soot nucleus production is decreased 10% nearly. Soot nucleus mass concentration is high in the area where the volatile concentration is high because volatile has not been burned out in time and formed soot nucleus. The secondary air may strengthen the mixture of gases in the furnace; reinforce the reaction between volatile and air. In the upper area in the furnace, mass concentration of soot nucleus is decreased.

Comparing to the experimental results that have been finished by authors, reduction of soot nucleus emission by secondary air, has same tendency.

Experiment introduction and result analysis

The experiment is carried out in a stoker-fired boiler. A batch of coal particles is approximately 7 kg. The fuel is the coal of power 2# which is used widely in the industrial boilers in Shanghai district. Ultimate and proximate analysis of the coal is shown in tab. 1. The coal was ignited on its surface by some burning charcoals soaked in kerosene.

Table 1. Ultimate and proximate analysis of coal

Proximate analysis [% , ar]				Ultimate analysis [% , ar]					Qnet ar [MJ/kg]
M	A	V	FC	C	H	S	N	O	
9.54	23.16	23.10	44.20	52.59	3.63	1.03	1.14	8.91	20.42

The secondary combustion air is located at 300 mm above the coal layer. The secondary air through four air-jet assemblies, opposing one another, is introduced as high velocity jets (approximately 22 m/s) normal to the axial (vertical) flow of the combustion gas. All air streams are measured with rotameters and introduced to the furnace at ambient temperature. The secondary air amount take up 20% of the total air that is varied according to the specified operating conditions. The total combustion air delivery is determined by the stoichiometric air requirement of the coal charge (based on coal composition and weight of coal charge) and the desired excess-air level. Typically, the total combustion-air delivery for the duration of the test is around 53 m^3 (at 10 °C and 1.01 bar). Measures of air distribution to the fuel bed in industrial traveling-grate stokers indicate that the primary and secondary combustion air to the fixed-grate model needed to be varied.

The experiment results also show that the smoke from coal combustion without secondary air is blacker than the smoke from coal combustion correlated with secondary air. It may be that the secondary air promotes the flue gases to mix with air and combust, decreases the condensation polymerization of coal volatile. Soot nucleus is the precursor of black smoke

formation. Less soot nucleus has been produced and less black smoke has been emission with secondary air injection.

Conclusions

Based on the simulation which include k-ε, combustion, radiation, and soot Tesner models, these conclusions can be drawn: the secondary air may reduce soot nucleus production; the highest mass concentration is reduced from $6.65 \cdot 10^{-11}$% to $6.00 \cdot 10^{-11}$%; and soot nucleus production is decreased 10% nearly. Black smoke emission control experiment in stoker-fired boiler has been done to prove that secondary air may reduce the soot nucleus production and black smoke emission.

References

[1] He, B. L., *et al*., Investigations on Mechanism of Soot Formation during Combustion and Control of Soot Emission, *Proceedings,* 5th International Symposium on Coal Combustion, Nanjing, China, 2003, pp. 1-5
[2] Wang-Hansen, C., *et al*., Kinetic Analysis of O_2 and NO_2 Based Oxidation of Synthetic Soot, *J. Phys. Chem. C, 117* (2013), 1, pp. 522-531
[3] Zhang, H. F., Nitrogen Evolution and Soot Formation during Secondary Coal Pyrolysis, Ph. D. thesis, Brigham Young University, Provo, Ut., USA, 2001
[4] Park, S., *et al*., A Model Development for Evaluating Soot-NO_x Interactions in a Blended 2-way Diesel Particulate Filter/Selective Catalytic Reduction, *Ind. Eng. Chem. Res.*, *51* (2012), 48, pp. 15582-15592
[5] Pahalagedara, L., *et al*., Structure and Oxidation Activity Correlations for Carbon Blacks and Diesel Soot, *Energy Fuels*, *26* (2012), 11, pp. 6757-6764
[6] Leistner, K., *et al.,* Impact of the Catalyst/Soot Ratio on Diesel Soot Oxidation Pathways, *Energy Fuels*, *26* (2012), 10, pp. 6091-6097
[7] Tan, M. J., Mao, J. X., The Advance Technologies of Coal-Fired Industrial Boiler in China, *Proceedings,* The Conference of the China-America Advanced Technologies of Industrial Boiler, Beijing, 2004, pp. 1-17
[8] Wu, Z. C., Wang, Q. C., Numerical Approach to Stefan Problem in a Two-Region and Limited Space, *Thermal Science*, *16* (2012), 5, pp. 1425-1430
[9] Tesner, P. A., *et al*., Kinetics of Dispersed Carbon Formation, *Combustion and Flame*, *17* (1971), pp. 253-260
[10] Fan, J., He, J.-H., Biomimic Design of Multi-Scale Fabric with Efficient Heat Transfer Property, *Thermal science*, *16* (2012), 5, pp. 1349-1352

Paper submitted: March 18, 2013
Paper revised: April 21, 2013
Paper accepted: April 22, 2013